Title

Regional Differences in the Coupling between Resting Cerebral Blood Flow and Metabolism may Indicate Action Preparedness as a Default State

Journal

Cerebral Cortex, 19(2)

ISSN

1047-3211

Authors

Gur, Ruben C

Ragland, J Daniel

Reivich, Martin

et al.

Publication Date

2009-02-01

DOI

10.1093/cercor/bhn087

Cerebral Cortex February 2009;19:375-382
doi:10.1093/cercor/bhn087
Advance Access publication June 4, 2008

Regional Differences in the Coupling between Resting Cerebral Blood Flow and Metabolism may Indicate Action Preparedness as a Default State

Ruben C. Gur[1,2,3], J. Daniel Ragland[1,4], Martin Reivich[3], Joel H. Greenberg[3], Abass Alavi[2,3] and Raquel E. Gur[1,2,3]

[1]Section of Neuropsychiatry, Department of Psychiatry and the Philadelphia Veterans Administration Medical Center Philadelphia, PA 19104, USA, [2]Department of Radiology, [3]Cerebrovascular Research Center of the Department of Neurology, University of Pennsylvania, Philadelphia, PA 19104, USA and [4]Current address: Imaging Research Center, Department of Psychiatry and Behavioral Sciences, University of California at Davis, Sacramento, CA 95817, USA

Although most functional neuroimaging studies examine task effects, interest intensifies in the "default" resting brain. Resting conditions show consistent regional activity, yet oxygen extraction fraction constancy across regions. We compared resting cerebral metabolic rates of glucose (CMRgl) measured with ^{18}F-labeled 2-fluoro-2-deoxy-D-glucose to cerebral blood flow (CBF) ^{15}O-H_2O measures, using the same positron emission tomography scanner in 2 samples ($n = 60$ and 30) of healthy right-handed adults. Region to whole-brain ratios were calculated for 35 standard regions of interest, and compared between CBF and CMRgl to determine perfusion relative to metabolism. Primary visual and auditory areas showed coupling between CBF and CMRgl, limbic and subcortical regions—basal ganglia, thalamus and posterior fossa structures—were hyperperfused, whereas association cortices were hypoperfused. Hyperperfusion was higher in left than right hemisphere for most cortical and subcallosal limbic regions, but symmetric in cingulate, basal ganglia and somatomotor regions. Hyperperfused regions are perhaps those where activation is anticipated at short notice, whereas downstream cortical modulatory regions have longer "lead times" for deployment. The novel observation of systematic uncoupling of CBF and CMRgl may help elucidate the potential biological significance of the "default" resting state. Whether greater left hemispheric hyperperfusion reflects lateral dominance needs further examination.

Keywords: functional neuroimaging, metabolic coupling, resting brain

Introduction

Most functional neuroimaging studies have focused on identifying neural networks activated by specific tasks (Brinkley and Rosse 2002; Friston et al. 2002) but Raichle et al. (2001) have pointed out the significance of the resting state as a "default mode of brain function." (p. 676) Definitions of the "resting state" vary; there has even been concern that a "resting brain state" is theoretically untenable and measurements of cerebral activity should only be done under structured task conditions (Buchsbaum et al. 1984). However, as several studies (Baron et al. 1982; Warach et al. 1987; Gur et al. 1995; Raichle 1998) have demonstrated, conditions where no specific tasks are given produce reliable and specific landscapes of metabolic activity. Furthermore, such resting measures have shown reliability of regional topography (Gur et al. 1987; Warach et al. 1987), and some regional variability has been related to habituation (Warach et al. 1992) and individual differences (Goldstein et al. 2002; Wang et al. 2002).

Relationships between rates of cerebral metabolism and blood flow have been examined in animals and humans and these values were shown to be tightly coupled (Reivich 1974). Studies in rats in which blood flow and glucose metabolism have been measured in the same animal (Lear et al. 1981), or in separate groups of animals (McCulloch et al. 1982; Frietsch et al. 2000) have shown an excellent correlation between blood flow and glucose metabolism. The animal data were derived from autoradiographic measurements using ligands labeled with radionuclides providing high spatial resolution. This strong correlation was observed in spite of a significant heterogeneity in capillary density throughout the brain (Klein et al. 1986). In humans, positron emission tomography (PET) studies have likewise reported high correlations among measures of metabolism and cerebral blood flow (CBF) (Baron et al. 1982; Fox et al. 1988; Bentourkia et al. 2000; Mintun et al. 2001).

Raichle et al. (2001; Raichle and Snyder 2007) pointed out that task-induced changes in blood flow are accompanied by smaller changes in oxygen consumption (Fox and Raichle 1986). This leads to decreased oxygen extraction fraction (OEF) from blood when blood flow increases, and an increase in oxygen extraction when blood flow decreases. Using PET with ^{15}O labeled water, Raichle et al. (2001) found a stable pattern of OEF during resting states, indicating deactivation mainly in visual areas when the eyes are closed. They interpreted the uniformity of OEF at rest to reflect an equilibrium "between the local metabolic requirements necessary to sustain a long-term modal level of neural activity and the level of blood flow in that region." (Raichle et al. 2001, pp. 677–678). Raichle et al. (2001) also pointed out that although task-induced activation occurs in a variety of regions depending on the task, specific regions become deactivated, relative to a resting baseline condition, across a range of tasks. They suggested that this network constitutes "an organized mode of brain function that is present as a baseline or default state and is suspended during specific goal-directed behaviors." (Raichle et al. 2001, p. 676). This hypothesis received considerable attention and support in recent studies (e.g., Mason et al. 2007; Shulman et al. 2007).

Notwithstanding the insights into the default brain state provided by examination of the OEF, we still "do not fully understand why the relationship between oxygen delivery and oxygen consumption changes during changes in brain activity" (Raichle et al. 2001, p. 677). Further understanding can be attained by examining the relationship between CBF and cerebral metabolic rates for glucose (CMRgl). It has long been recognized that the brain uses glucose as a metabolic substrate almost exclusively, for energetic and even biosynthetic needs (Siesjö 1978; Sokoloff 1981; Clarke and Sokoloff 1999; Nehlig and Coles 2007). Indeed, an abundant supply of glucose through CBF is vital for brain function, as evidenced by nearly instantaneous unconsciousness induced by supply interruption

(Clarke and Sokoloff 1999). Furthermore, "[i]n the resting brain, oxygen is almost entirely used for the oxidation of glucose with only a small excess of glucose being metabolized to lactate as a final product" (Nehlig and Coles 2007, p. 1239). Task-related activation is associated with much smaller oxygen consumption increases than either CBF or CMRgl (~5% compared with ~54%, see Fox and Raichle 1986; Fox et al. 1988). Examining the relationship between CBF and CMRgl could help explain the excess CBF relative to oxygen metabolism increase associated with activation. Comparison of such values at a resting state could help determine whether the coupling between CBF and CMRgl is uniform across regions, as is the case for OEF, or whether there are regions that are either hyperperfused or hypoperfused at a resting state, relative to CMRgl. With a larger CMRgl compared with oxygen metabolism increase during activation, and an estimated average extraction fraction of glucose from the blood being about 8% (Hawkins et al. 1983), we hypothesized that the CMRgl coupling with CBF will not be as uniform as for oxygen metabolism. Specifically, resting hyperperfusion would confer advantage to regions that are at the "frontline" of the information-processing cascade, such as subcortical limbic areas, whereas regions involved in downstream modulation could afford relative hypoperfusion at rest. Both CMRgl and CBF have been measured with PET, using ^{18}F-fluoro-deoxyglucose and ^{15}O labeled water respectively, and we compared region to whole-brain (R/WB) ratios of resting CBF with CMRgl in a standard set of regions of interest (ROIs).

Materials and Methods

Participants

Data were examined from healthy participants in previously published studies, which yielded 2 data sets. The first consisted of resting baseline measures of CMRgl assessed with the ^{18}F-FDG (^{18}F-labeled 2-fluoro-2-deoxy-D-glucose) method and published in Gur et al. (1995). That sample included 60 healthy volunteers (37 men, 23 women), age ± SD 27.5 ± 6.8 years (range 18.1–44.1), and 14.6 ± 2.0 years of education. The second data set consisted of resting baseline measures of CBF determined with the ^{15}O-H_2O "ramped infusion" method (Ragland et al. 1997). The sample included 30 healthy subjects (16 men, 14 women), 26.3 ± 6.3 years old (range 18.3–43.4), with 15.3 ± 1.9 years of education. All participants were right-handed (Raczkowski et al. 1974).

The same recruitment and assessment procedures were applied in both studies. Participants were recruited through advertisements in the community and underwent medical, neurological and psychiatric evaluation, including a structured interview, and laboratory tests. Individuals with a history of any illnesses affecting brain function, such as head trauma with loss of consciousness and substance use, were excluded. The protocol was approved by the institutional review board and written informed consent was obtained from each participant after the nature and possible consequences of the study were explained.

Procedures

Participants were all scanned in the morning after an overnight fast and placed in the scanner in a supine position. Studies began by cannulating a radial artery under local anesthesia with 2% xylocaine. A venous line was placed in the contralateral antebrachium. Both lines were kept patent with solutions of physiological saline. Imaging was performed on the UGM 240H volume imaging scanner (Smith et al. 1994), with a 12.8 cm axial field of view and spatial resolution of 5.5-mm full width half maximum in all directions (UGM Medical Systems, Philadelphia, PA) (Karp et al. 1993). Participants' heads were aligned along the orbitomeatal line and manual head holder restraints reduced movement. During resting baseline scans participants were recumbent in a quiet, dimly lit room for the FDG study and in the scanner for the CBF study. In both they were with eyes open and ears unoccluded, and instructed to stay quiet and relaxed without either exerting mental effort or falling asleep.

Measures of CMRgl with ^{18}F-FDG

Approximately, 185 MBq (5 mCi) of FDG were administered intravenously. To determine the input function, arterial samples were obtained over 90 min. Activity of ^{18}F in 250-μL aliquots was measured in a dose calibrator. Image acquisition began 40 min after isotope administration. Tissue activity concentration per unit time was calculated using scanner calibration and dead time correction factors. Together with calibrated blood activity concentration values, metabolism was calculated using lumped and rate constants (Reivich et al. 1985).

Measures of CBF with ^{15}O-H_2O

Participants received intravenous injections of ^{15}O-water using a modified bolus ramped infusion technique (Lammertsma et al. 1981; Smith et al. 1995). A programmed infusion of approximately 1665 MBq (45 mCi) of ^{15}O-water was delivered over 3.3 min. This results in rapid elevation of tissue activity to the peak of the count rate capability of the camera. The measuring period continued over 4.21 min., and dynamic scans were obtained continuously. Tissue activity concentrations peak over the first 1.5 min of the measurement period and then level off because of increased washout (Smith et al. 1995). To determine the input function, arterial blood samples were obtained through a 3-way stopcock coupled to the arterial catheter. The arterial concentration of radioactivity was measured from 0.25-mL aliquots of whole blood in a calibrated (6.4 kcps/mCi) NaI(Tl) well counter (Tennelec 707, Memphis, TN). Aliquots of spun plasma were measured as a cross check, but the whole blood values were used in the calculations.

Image Processing and Statistical Analysis

PET scans from the CMRgl and CBF studies were processed identically. They were corrected for attenuation, scatter, and dead time, and were cross-registered with corresponding magnetic resonance images (MRI) using established procedures (Gur et al. 1987, 1995; Ragland et al. 1997). Templates with ROIs were custom fitted to MRI slices by investigators trained to an inter-rater reliability criterion of >0.85 (intraclass correlation) for 39 of the 42 regions, and of these, 35 with reliability > 0.90 were included in the statistical analysis. Figure 1 illustrates the regional boundaries for the ROIs.

R/WB ratios were calculated based on the absolute metabolic rates and CBF values. A Generalized Estimating Equations (GEE) logistic regression (SAS Procedure Genmod) model, that accommodates multiple nonindependent measurements without requiring sphericity, was employed for data analysis with one between-group factor (CMRgl vs. CBF) and one within-group factor (region). To contain type-I (experimenter-wise) error probability, the analyses were done for 8 groups of regions as follows: 1) frontal: superior frontal; dorsal prefrontal—lateral; dorsal prefrontal—medial; mid-frontal; inferior frontal. 2) Parietal: sensorimotor; superior parietal; supramarginal gyrus. 3) Occipital: occipital cortex, lateral; occipital cortex, medial; lingual gyrus; fusiform gyrus. 4) Temporal: occipital temporal; superior temporal; mid-temporal; inferior temporal; temporal pole. 5) Limbic: parahippocampal gyrus; hippocampus; amygdala; insula; orbital frontal; rectal gyrus; cingulate gyrus—anterior; cingulate gyrus—genu; cingulate gyrus—posterior. 6) Corpus callosum: anterior; posterior. 7) Basal ganglia–hypothalamus: caudate nucleus; lenticular—medial (globus pallidus); lenticular—lateral (putamen); thalamus. 8) Somatomotor: midbrain; pons; cerebellum. To examine effects of laterality, follow-up GEE analyses were performed adding hemisphere as a within factor. To contain type-I error, we first tested for the significance of the measure × hemisphere interaction, relevant to the issue of CBF/CMRgl coupling, and if that was significant we tested higher-order measure × hemisphere × region interactions.

Results

The regional resting baseline values for CMRgl and CBF in each hemisphere are presented in Table 1. As expected, regions with

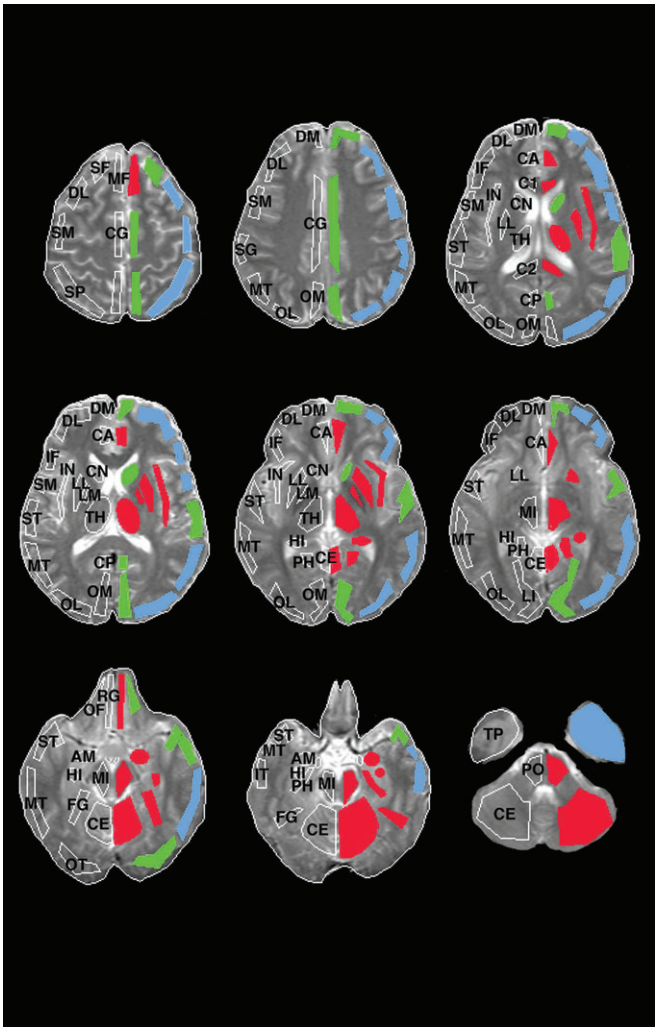

Figure 1. Placement of representative ROIs on MR images. The following regions were examined (abbreviations on left hemispheres): superior frontal (SF), dorsolateral prefrontal (DL), dorsomedial prefrontal (DM), mid-frontal (MF), inferior frontal (IF), sensorimotor (SM), superior parietal (SP), supramarginal gyrus (SG), occipital—medial (OM), occipital—lateral (OL), lingual gyrus (LI), fusiform gyrus (FG), occipital temporal (OT), superior temporal (ST), mid-temporal (MT), inferior temporal (IT), temporal pole (TP), parahippocampal gyrus (PH), hippocampus (HI), uncus (UN), amygdala (AM), insula (IN), orbital frontal (OF), rectal gyrus (RG), cingulate gyrus—anterior (CA), cingulate gyrus (CG), cingulate gyrus—posterior (CP), corpus callosum—anterior (C1), corpus callosum—posterior (C2), caudate nucleus (CN), lenticular—medial (globus pallidus) (LM), lenticular—lateral [putamen] (LL), thalamus (TH), midbrain (MI), pons (PO), cerebellum (CE). The color-coding on the right hemisphere is based on the results (see Results section) and indicates hyperperfusion (red), hypoperfusion (blue) and coupling (green).

higher metabolic activity also had generally higher CBF. This was reflected in a cross-sample correlation of $r = 0.563$, df = 33, $P = 0.0004$. A scatterplot of regional values for CMRgl and CBF (Fig. 2) indicates a smooth relationship across the range of values, with greater inter-regional variability in CBF (average variance of 0.0801 ± 0.0292 for CBF compared with 0.022 ± 0.0081 for CMRgl, $t = 10.71$, df = 31.3, $P < 0.0001$ [degrees of freedom were Satterthwaite corrected for unequal variance because $F = 12.81$, df = 29,59, $P < 0.0001$]). Notably, the amygdala (appearing as an outlier above the identity line in Fig. 2) has disproportionately higher CBF than expected from its CMRgl, and when it is removed the inter-regional correlation improves to $r = 0.653$, df = 32, $P < 0.0001$.

The GEE comparing resting CMRgl and CBF for the frontal regions showed no main effect of measure, χ^2 (1) = 0.85, $P = 0.3563$, but a strong main effect of region, χ^2 (4) = 52.51, $P < 0.0001$ and a region × measure interaction, χ^2 (3) = 27.42, $P < 0.0001$, indicating that the effect was not uniform across regions. All frontal regions showed relative hypoperfusion except for the mid-frontal region, which showed marked hyperperfusion. The parietal regions showed main effects of measure, χ^2 (1) = 7.75, $P = 0.0054$, CBF lower than CMRgl; region, χ^2 (2) = 41.63, $P < 0.0001$, and a region × measure interaction, χ^2 (2) = 12.41, $P = 0.0020$, indicating that here too the effect was not uniform across regions. Specifically, all parietal regions showed hypoperfusion, but it was most pronounced in the superior parietal compared with sensorimotor and supramarginal regions. The occipital regions showed no main effect of measure, χ^2 (1) = 0.55, $P = 0.4594$, but a large main effect for region, χ^2 (3) = 56.90, $P < 0.0001$; and a region × measure interaction, χ^2 (2) = 31.42, $P < 0.0001$, indicating that here too the effect was not uniform across regions. The medial occipital and lingual gyrus showed tight coupling between CBF and CMRgl, the lateral occipital region was hypoperfused, whereas the fusiform gyrus showed about equally marked hyperperfusion. The temporal regions showed a main effect of measure, χ^2 (1) = 6.67, $P = 0.0098$, indicating overall hypoperfusion. There was a main effect for region, χ^2 (4) = 49.59, $P < 0.0001$; and a region × measure interaction, χ^2 (4) = 33.70, $P < 0.0001$. The interaction indicated that although 2 temporal regions (occipito-temporal and superior temporal gyrus) showed coupling between CBF and CMRgl, all other temporal cortex regions showed hypoperfusion. For limbic regions, the main effect of measure was significant in the opposite direction, with CBF higher than CMRgl, χ^2 (1) = 24.57, $P < 0.0001$. There was a main effect for region, χ^2 (8) = 54.23, $P < 0.0001$; and a region × measure interaction, χ^2 (8) = 48.33, $P < 0.0001$. The interaction indicated that relative hyperperfusion in limbic areas was attenuated in orbital frontal cortex and the genu and posterior cingulate gyrus. For the corpus callosum, the main effect of measure was significant in the direction of relatively higher CBF than CMRgl, χ^2 (1) = 19.53, $P < 0.0001$. The main effect for region and region × measure interactions were not significant (χ^2 (1) = 2.39, $P = 0.1219$ and χ^2 (1) = 0.01, $P = 0.9932$, respectively). For the basal ganglia and thalamus, there were main effects of measure, χ^2 (1) = 6.80, $P = 0.0091$, with CBF higher than CMRgl, region, χ^2 (3) = 46.48, $P < 0.0001$, and a region × measure interaction, χ^2 (3) = 31.78, $P < 0.0001$. The interaction indicated that although the caudate nucleus was only mildly hyperperfused, the lenticular nuclei and thalamus showed pronounced hyperperfusion. For the somatomotor regions, there was again a main effect of measure, with CBF higher than CMRgl, χ^2 (1) = 18.78, $P < 0.0001$. There was a main effect for region, χ^2 (2) = 45.41, $P < 0.0001$; and a region × measure interaction, χ^2 (2) = 8.47, $P = 0.0017$. The interaction indicated that hyperperfusion was somewhat diminished in the pons and cerebellum relative to midbrain. The regional distribution of hyperperfused and hypoperfused regions is illustrated in Figure 1, with hyperperfused regions (i.e., significantly higher CBF than CMRgl) in red, hypoperfused regions in blue, and coupled regions in green.

The GEE examining laterality effects showed for the frontal regions both a hemisphere × measure, χ^2 (1) = 32.07, $P < 0.0001$, and a hemisphere × measure × region interaction, χ^2 (8) = 42.12, $P < 0.0001$. To clarify this and subsequent 3-way

Table 1
Regional hemispheric means and SDs for CMRgl and CBF in R/WB ratios (region abbreviations as in Fig. 1)

	Brodmann area	CMRgl (n = 60)				CBF (n = 30)			
		Left		Right		Left		Right	
		Mean	SD	Mean	SD	Mean	SD	Mean	SD
SF	6,8,9	0.94	0.10	0.95	0.14	0.96	0.14	0.83	0.14
DL	9,10,46	1.03	0.08	1.03	0.10	1.08	0.12	0.86	0.11
DM	6,8,9,10	0.94	0.07	0.94	0.08	1.01	0.14	0.90	0.10
MF	6,8,10,32	1.16	0.12	1.08	0.13	1.34	0.26	1.24	0.16
IF	44,45,46,47	1.09	0.09	1.07	0.10	1.13	0.13	0.90	0.11
SM	1,2,3,4,6,40,43	1.10	0.08	1.05	0.11	1.09	0.14	0.88	0.10
SP	7,40	1.03	0.11	0.99	0.13	0.89	0.12	0.78	0.10
SG	40	1.01	0.11	0.97	0.12	0.97	0.15	0.82	0.14
OM	17,18,19	1.16	0.10	1.10	0.11	1.20	0.12	1.09	0.07
OL	18,19	0.89	0.10	0.93	0.10	0.80	0.06	0.73	0.05
LI	17,18,19	1.11	0.14	1.09	0.15	1.15	0.14	1.06	0.15
FG	19,37	1.05	0.14	1.09	0.14	1.32	0.26	1.15	0.23
OT	17,18,19	0.97	0.14	0.98	0.15	1.00	0.18	0.94	0.18
ST	12,22,38,42	1.09	0.07	1.06	0.10	1.18	0.11	0.97	0.09
MT	19,21,22,37,39	1.04	0.07	1.04	0.09	0.97	0.08	0.84	0.08
IT	20,21,37	1.08	0.16	1.02	0.18	1.03	0.18	0.83	0.11
TP	20,21,28,34,36,38	0.98	0.20	1.03	0.21	0.89	0.15	0.82	0.13
PH	27,28,30,35,36	0.99	0.09	1.04	0.10	1.29	0.18	1.25	0.17
HI		0.97	0.09	0.96	0.10	1.32	0.19	1.21	0.15
AM		0.90	0.13	0.91	0.13	1.49	0.33	1.47	0.28
IN		1.11	0.07	1.23	0.08	1.53	0.20	1.39	0.19
OF	10,11	1.08	0.14	1.09	0.15	1.23	0.26	1.00	0.17
RG	11	1.16	0.17	1.16	0.15	1.68	0.40	1.52	0.33
CA	24,32	1.11	0.09	1.04	0.10	1.53	0.15	1.37	0.20
CG	23,24,31	1.15	0.16	0.95	0.16	1.20	0.23	1.08	0.23
CP	23,29,30,31	1.21	0.19	1.14	0.14	1.35	0.20	1.25	0.17
C1		0.79	0.09	0.78	0.09	0.88	0.20	0.86	0.17
C2		0.86	0.16	0.76	0.11	0.96	0.18	0.85	0.18
CN		1.14	0.08	1.15	0.09	1.22	0.22	1.23	0.23
LM		1.10	0.08	1.21	0.10	1.36	0.24	1.55	0.27
LL		1.21	0.08	1.27	0.08	1.58	0.27	1.63	0.24
TH		1.09	0.07	1.10	0.08	1.34	0.20	1.37	0.20
MI		0.98	0.12	0.95	0.11	1.31	0.22	1.31	0.20
PO		0.88	0.16	0.83	0.16	1.13	0.19	1.06	0.19
CE		0.95	0.11	1.02	0.14	1.24	0.14	1.23	0.13

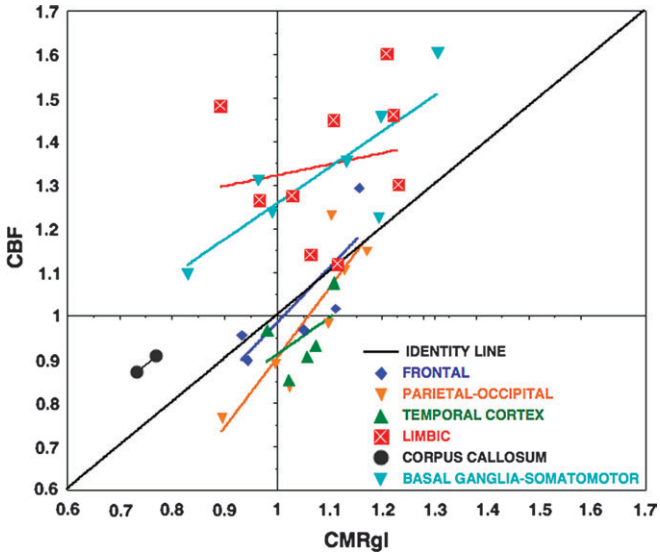

Figure 2. An intergroup scatterplot of regional CMRgl (x-axis) and CBF (y-axis) values, with regression and identity lines. The color-coding indicates regional membership (Frontal = blue diamonds; parietal–occipital = orange downward pointing triangles; Temporal = green upward pointing triangles; Limbic = red squares; corpus callosum = black circles; basal ganglia and somatomotor regions = turquoise downward pointing triangles). Regression lines were calculated separately for each grouping.

interactions, Figure 3 displays the CBF/CMRgl ratios for each hemisphere, where hyperperfusion is indicated by distance from unity. As can be seen in Figure 3, the average frontal hypoperfusion is largely driven by the right hemispheric values. The left hemisphere throughout most frontal regions was more highly perfused than the right. The exception was the mid-frontal region, which was hyperperfused bilaterally. The parietal regions also showed both hemisphere × measure, χ^2 (1) = 17.36, $P < 0.0001$, and a hemisphere × measure × region interaction, χ^2 (4) = 19.28, $P = 0.0007$. As can be seen in Figure 3, although the parietal lobe was hypoperfused overall, the left hemisphere was less so especially in sensorimotor cortex. The occipital regions showed both hemisphere × measure, χ^2 (1) = 23.02, $P < 0.0001$, and a hemisphere × measure × region interaction, χ^2 (6) = 37.83, $P < 0.0001$. As can be seen in Figure 3, left hemispheric ratios were higher in most regions but especially in fusiform gyrus. The temporal regions likewise showed both hemisphere × measure, χ^2 (1) = 25.18, $P < 0.0001$, and a hemisphere × measure × region interaction, χ^2 (8) = 39.64, $P < 0.0001$. The interaction indicated that although one temporal region (occipito-temporal) showed bilateral coupling between CBF and CMRgl, all other temporal cortex regions showed less hypoperfusion on the left. Notably, superior temporal gyrus was hyperperfused on the left and hypoperfused on the right. For limbic regions, there were both hemisphere × measure, χ^2 (1) = 31.05, $P < 0.0001$, and hemisphere × measure × region interactions, χ^2 (16) = 51.49, $P < 0.0001$. The interactions indicate that although the left

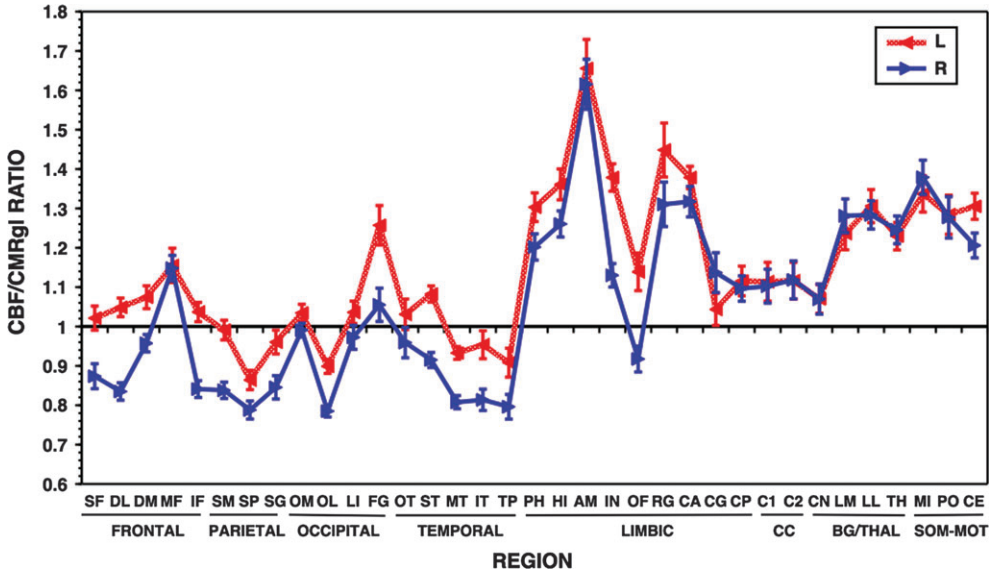

Figure 3. Mean (±SEM) of the ratios of relative regional CBF to glucose metabolism (CMRgl) in frontal, parietal, occipital, temporal, limbic, corpus callosum (CC), basal ganglia, and thalamus (BG/THAL), and posterior fossa somatomotor (SOM-MOT) areas. Region placement is shown in Figure 1, where the regional labels are spelled out in the legend. The error bars represent the standard error of the mean for ratios, defined as the relative standard error (RSE) multiplied by the ratio. RSE is standard error relative to the mean; the RSE squared of (x/y) is equal to the sum of the RSEs squared of x and of y, following which the absolute SE of (x/y) is simply RSE (x/y) times (x/y).

hemisphere was consistently hyperperfused relative to the right, this effect varied by region. It was pronounced for insula and orbitofrontal cortex, and nearly absent in the amygdala and cingulate regions. For the corpus callosum, the hemisphere × measure interaction was not significant, χ^2 (1) = 0.00, P = 0.9624. For the basal ganglia and thalamus, as well as for the somatomotor regions, the hemisphere × measure interaction was not significant, χ^2 (1) = 0.33, P = 0.5672 and χ^2 (1) = 1.55, P = 0.2136, respectively. As can be seen in Figure 3, these regions are all hyperperfused bilaterally.

Discussion

The results indicate overall coupling between cerebral glucose metabolism and blood flow in the resting brain, consistent with earlier studies (Reivich 1974; Raichle et al. 2001). However, as hypothesized, some regions are significantly hyperperfused, with higher relative CBF than CMRgl, whereas others are hypoperfused. The topographic distribution of these regions does not seem random. Primary visual and auditory areas showed coupling between CBF and CMRgl, limbic and subcortical regions—basal ganglia, thalamus, and posterior fossa structures—were hyperperfused, whereas association cortices were hypoperfused. Given their role in arousal and early stages of stimulus encoding, limbic regions (Pourtois and Vuilleumier 2006), thalamus (Aguilar and Castro-Alamancos 2005), and posterior fossa (Schmahmann and Pandya 1995; Ackermann et al. 2007) have in common the potential need for precipitous and rapid activation. By contrast, regions showing hypoperfusion are in association or modulatory cortices, where deployment occurs downstream and is hence more gradual and predictable. The need for rapid deployment in basal ganglia, which are markedly hyperperfused, may reflect their important limbic contributions in ventral portions of the putamen, globus pallidus, and caudate, as well as basal forebrain, which may be especially important for arousal and attention (e.g., Mogenson et al. 1980; Floresco et al. 2001; Chudasama and Robbins 2006). These results extend Raichle et al. (2001) view of the resting state as a default mode of brain function, suggesting an adaptive anticipatory uncoupling between blood flow and glucose metabolism.

Other lines of research support this hypothesis, including evidence that there is a regional increase in oxygen metabolism prior to any increase in regional blood flow. Specifically during sensory stimulation, changes in local oxygen metabolism appear to precede changes in local CBF. Microelectrode studies in the rat during electrical stimulation of the forepaw show that the metabolic response occurs almost 1 second prior to the blood flow response (Ances et al. 2001), consistent with optical measurements of oxygen and cerebral blood hemodynamics during visual activation in the cat (Malonek and Grinvald 1996). Over the past decade a preponderance of studies in animals and humans using optical imaging, microelectrodes, magnetic resonance spectroscopy, and functional magnetic resonance imaging have observed what has become known as the "initial dip," or an increase in deoxyhemoglobin that precedes any changes in cerebral hemodynamics (Ances 2004). These studies indicate that in response to stimulation or task demands, neuronal activity increases prior to any increases in blood flow or blood volume. In regions where a quick response to a stimulus would be beneficial, resting hyperperfusion would be the adaptive anticipatory metabolic state.

The hypothesis is further supported by examination of variability within regions, reflected by the measure × region interactions. Although most frontal regions showed hypoperfusion, the medial frontal cortex was quite strongly hyperperfused. This may reflect the central role of this region in motor functions, particularly related to speed (Sawle et al. 1991). Our results suggest that the medial frontal area has both high metabolic activity (among the highest of all cortical regions) and an excess of CBF, further supporting its potential role as contributing "to the neural instantiation of aspects of the multifaceted 'self.'"(Raichle et al. 2001; see also Gusnard et al. 2001). Values in the parieto-occipital area seem to adhere to the same principle. The parietal regions, which serve as

association cortex, are all hypoperfused, whereas variability is seen in occipital cortex. The medial occipital region, containing primary visual cortex, has high CMRgl but comparable CBF ratios, reflecting tight coupling, whereas the lateral occipital region, containing secondary visual association cortex, is pronouncedly hypoperfused. Our participants had their eyes open, but were studied in a dimly lit room with no stimulation. This differs from participants in Raichle et al., who were studied with eyes closed. Our findings thus support Raichle et al.'s (2001) hypothesis that "the baseline state of these [visual] areas is more nearly approximated when subjects rest quietly with their eyes open." (p. 680). The fusiform cortex, which plays an early role in the processing of complex spatial layouts, including faces (e.g., Downing et al. 2006; Iidaka et al. 2006), is substantially hyperperfused. Within limbic regions, consistent with their role in modulating emotional behavior, the orbital frontal cortex and the genu and posterior cingulate areas show less hyperperfusion than the phylogenetically older regions such as parahippocampal gyrus, hippocampus, and, in particular, the amygdala. Notably, the amygdala stands out as having the highest rate of CBF relative to CMRgl. This is consistent with its role in the processing of threat-related stimuli (Kluver and Bucy 1939; Damasio et al. 2000; Amaral 2003; Etkin et al. 2004; Coccaro et al. 2007). The corpus callosum is hyperperfused in both anterior and posterior sections, as are the basal ganglia and posterior fossa regions. The marked hyperpefusion in the posterior fossa somatomotor regions contrasts with the hypoperfusion in sensorimotor cortex, again suggesting that hypoperfusion characterizes regions that may have a greater lag time for activation.

The laterality effects indicated higher CBF/CMRgl ratios in the left hemisphere throughout most cortical regions, and bilaterally symmetric hyperperfusion in the cingulate, corpus callosum, basal ganglia, thalamus, and somatomotor regions. In this sample of right-handed individuals, the finding is consistent with the hypothesis that higher ratios indicate greater preparedness for deployment. The laterality finding, however, was not hypothesized and should be further examined in future studies.

The results of this study must be considered within the context of its methodological limitations. First, the 2 groups of subjects were studied in somewhat different environments. The tracer uptake for FDG was done in a quiet dimly lit room, whereas the CBF studies involved lying in a scanner with the subject's head positioned within the scanner bore. A more precise estimation of discrepancies between CMRgl and CBF could be obtained had resting values been available for both measures in the same sample under identical conditions. Such data would also permit examination of individual differences in the degree of CMRgl and CBF coupling during a resting state. It is noteworthy, however, that in spite of coming from different samples, the regional values showed rather prominent correspondence between CMRgl and CBF, supporting overall coupling. Other limitations of the method include failure to discern several physiological and technical factors that could introduce regional differential sensitivity such as proximity to large arteries, differential density of vascularization, differential partial volume effects, and differential resolution of ^{15}O and ^{18}F isotopes. Thus, given that limbic and midbrain structures are on the medial aspect of the brain and may be in close proximity to large vessels, this factor might be responsible, at least in part, for the higher apparent hyperperfusion in these regions. The results are also limited in that we have used a standard preselected set of ROIs. Applying statistical parametric analysis could reveal more clearly the distributed network of regions associated with hyper- or hypoperfusion. Such analysis could also allow more direct comparability between perfusion status relative to CMRgl and the distribution of regions implicated in the default network (Raichle et al. 2001). Some regions showing hyperperfusion in our study, such as hippocampus, rectal gyrus and amygdala, are part of the default network, whereas the medial occipital region has equal CMRgl and CBF. For cortical regions it would have been especially helpful to have voxel-wise data to determine comparability with other studies of the default network. We are in the process of transferring the PET data to a platform that would permit such analyses. Finally, there could be alternative explanations and reasons for the observed variability in the ratio of cerebral perfusion to glucose metabolic rates. In addition to regional variability in capillary density (Klein et al. 1986), the effects could relate to differences in carotid versus vertebrobasilar circulatory systems, regional differences in neurochemical innervation (e.g., cholinergic, noradrenergic), or intrinsic neurochemical innervation (e.g., gamma-aminobutyric acid, glutamate). The present methodology does not permit resolution of these explanations and further research is required.

Notwithstanding these limitations, the results offer strong support for the merit of functional imaging investigations of the resting landscape of brain metabolic activity. Our results extend Raichle et al.'s hypothesis of a default brain state, based on the uniformity of OEF across regions at the resting state. When CMRgl, which shows greater task-induced changes than oxygen metabolism, is compared with CBF, the results suggest that such a default state may also reflect readiness for action, probably of evolutionary significance. They reveal a novel relation between cerebral metabolism and blood flow at a "default" resting state, with systematic variation among brain regions in the degree to which they are hyper- or hypoperfused relative to metabolic demands. Regions related to arousal and early stages of stimulus processing, including evaluation of their threat potential, where action can be unpredictable, have excess CBF relative to CMRgl. By contrast, regions implicated in secondary association, downstream emotional modulation and executive processes have relatively less CBF compared with CMRgl. The extent to which hyperperfusion relative to CMRgl changes as a result of task-related activation can be determined in future studies. Such work can help clarify whether there is a consistent set of regions that show similar changes across all tasks, as Raichle et al have suggested based on OEF results. Finally, it would be interesting to examine whether this principle operates across species. Although the amygdala, basal ganglia and posterior fossa structures would likely show hyperperfusion across species, differences may be observed related to species-specific salience of modulatory systems.

Funding

Grants (MH-64045 and MH-60722).

Notes

We thank Steven E. Arnold, Graham J. Kemp, the late John S. Leigh, and Marcus E. Raichle for useful discussions and the PET Center staff for their invaluable help. *Conflict of Interest*: None declared.

Address correspondence to Ruben C. Gur, PhD, Neuropsychiatry, 10th floor Gates Bldg., University of Pennsylvania, 3400 Spruce St., Philadelphia, PA 19104-4283, USA. Email: gur@upenn.edu.

References

Ackermann H, Mathiak K, Riecker A. 2007. The contribution of the cerebellum to speech production and speech perception: clinical and functional imaging data. Cerebellum. 6:202–213.

Aguilar JR, Castro-Alamancos MA. 2005. Spatiotemporal gating of sensory inputs in thalamus during quiescent and activated states. J Neurosci. 25:10990–11002.

Amaral DG. 2003. The amygdala, social behavior, and danger detection. Ann N Y Acad Sci. 1000:337–347.

Ances BM. 2004. Coupling of changes in cerebral blood flow with neural activity: what must initially dip must come back up. J Cereb Blood Flow Metab. 24:1–6.

Ances BM, Buerk DG, Greenberg JH, Detre JA. 2001. Temporal dynamics of the partial pressure of brain tissue oxygen during functional forepaw stimulation in rats. Neurosci Lett. 306: 106–110.

Baron JC, Lebrun-Grandie P, Collard P, Crouzel C, Mestelan G, Bousser MG. 1982. Noninvasive measurement of blood flow, oxygen consumption, and glucose utilization in the same brain regions in man by positron emission tomography: concise communication. J Nucl Med. 23:391–399.

Bentourkia M, Bol A, Ivanoiu A, Labar D, Sibomana M, Coppens A, Michel C, Cosnard G, De Volder AG. 2000. Comparison of regional cerebral blood flow and glucose metabolism in the normal brain: effect of aging. J Neurol Sci. 181:19–28.

Brinkley JF, Rosse C. 2002. Imaging and the Human Brain Project: a review. Methods Inf Med. 41:245–260.

Buchsbaum MS, Cappelletti J, Ball R, Hazlett E, King AC, Johnson J, Wu J, DeLisi LE. 1984. Positron emission tomographic image measurement in schizophrenia and affective disorders. Ann Neurol. 15(Suppl):S157–S165.

Chudasama Y, Robbins TW. 2006. Functions of frontostriatal systems in cognition: comparative neuropsychopharmacological studies in rats, monkeys and humans. Biol Psychol. 73:19–38.

Clarke DD, Sokoloff L. 1999. Circulation and energy metabolism. In: Siegel GJ, Agranoff BW, Albers RW, Fisher SK, Uhler MD, editors. Basic neurochemistry: molecular, cellular, and clinical aspects. 6th ed. New York: Raven Press. p. 637–669.

Coccaro EF, McCloskey MS, Fitzgerald DA, Phan KL. 2007. Amygdala and orbitofrontal reactivity to social threat in individuals with impulsive aggression. Biol Psychiatry. 62:168–178.

Damasio AR, Grabowski TJ, Bechara A, Damasio H, Ponto LL, Parvizi J, Hichwa RD. 2000. Subcortical and cortical brain activity during the feeling of self-generated emotions. Nat Neurosci. 3:1049–1056.

Downing PE, Chan AW, Peelen MV, Dodds CM, Kanwisher N. 2006. Domain specificity in visual cortex. Cereb Cortex. 16:1453–1461.

Etkin A, Klemenhagen KC, Dudman JT, Rogan MT, Hen R, Kandel ER, Hirsch J. 2004. Individual differences in trait anxiety predict the response of the basolateral amygdala to unconsciously processed fearful faces. Neuron. 44:1043–1055.

Floresco SB, Blaha CD, Yang CR, Phillips AG. 2001. Modulation of hippocampal and amygdalar-evoked activity of nucleus accumbens neurons by dopamine: cellular mechanisms of input selection. J Neurosci. 21:2851–2860.

Fox PT, Raichle ME. 1986. Focal physiological uncoupling of cerebral blood flow and oxidative metabolism during somatosensory stimulation in human subjects. Proc Natl Acad Sci USA. 83: 1140–1144.

Fox PT, Raichle ME, Mintun MA, Dence C. 1988. Nonoxidative glucose consumption during focal physiologic neural activity. Science. 241: 462–464.

Frietsch T, Krafft P, Piepgras A, Lenz C, Kuschinsky W, Waschke KF. 2000. Relationship between local cerebral blood flow and metabolism during mild and moderate hypothermia in rats. Anesthesiology. 92:754–763.

Friston KJ, Glaser DE, Henson RN, Kiebel S, Phillips C, Ashburner J. 2002. Classical and Bayesian inference in neuroimaging: applications. Neuroimage. 16:484–512.

Goldstein RZ, Volkow ND, Chang L, Wang GJ, Fowler JS, Depue RA, Gur RC. 2002. The orbitofrontal cortex in methamphetamine addiction: involvement in fear. Neuroreport. 13:2253–2257.

Gur RC, Gur RE, Obrist WD, Skolnick BE, Reivich M. 1987. Age and regional cerebral blood flow at rest and during cognitive activity. Arch Gen Psychiatry. 44:617–621.

Gur RC, Mozley LH, Mozley PD, Resnick SM, Karp JS, Alavi A, Arnold SE, Gur RE. 1995. Sex differences in regional cerebral glucose metabolism during a resting state. Science. 267:528–531.

Gusnard DA, Akbudak E, Shulman GL, Raichle ME. 2001. Medial prefrontal cortex and self-referential mental activity: relation to a default mode of brain function. Proc Natl Acad Sci USA. 98:4259–4264.

Hawkins RA, Mans AM, Davis DW, Vina JR, Hibbard LS. 1983. Glucose availability to individual cerebral structures is correlated to glucose metabolism. J Neurochem. 40:1013–1018.

Iidaka T, Matsumoto A, Haneda K, Okada T, Sadato N. 2006. Hemodynamic and electrophysiological relationship involved in human face processing: evidence from a combined fMRI-ERP study. Brain Cogn. 60:176–186.

Karp JS, Kinahan PE, Muehllehner G, Countryman P. 1993. Effect of increased axial field of view on the performance of a volume PET scanner. IEEE Trans Med Imaging. 12:299–306.

Klein B, Kuschinsky W, Schrock H, Vetterlein F. 1986. Interdependency of local capillary density, blood flow, and metabolism in rat brains. Am J Physiol. 251:H1333–H1340.

Kluver H, Bucy PC. 1939. Preliminary analysis of functions of the temporal lobes in monkeys. Arch Neurol Psychiatry. 42:979–1000.

Lammertsma AA, Jones T, Frackowiak RS, Lenzi GL. 1981. A theoretical study of the steady-state model for measuring regional cerebral blood flow and oxygen utilisation using oxygen-15. J Comput Assist Tomogr. 5:544–550.

Lear JL, Jones SC, Greenberg JH, Fedora TJ, Reivich M. 1981. Use of 123I and 14C in a double radionuclide autoradiographic technique for simultaneous measurement of lCBF and lCMRgl. Theory and method. Stroke. 12:589–597.

Malonek D, Grinvald A. 1996. Interactions between electrical activity and cortical microcirculation revealed by imaging spectroscopy: implications for functional brain mapping. Science. 272:551–554.

Mason MF, Norton MI, Van Horn JD, Wegner DM, Grafton ST, Macrae CN. 2007. Wandering minds: the default network and stimulus-independent thought. Science. 315:393–395.

McCulloch J, Kelly PA, Ford I. 1982. Effect of apomorphine on the relationship between local cerebral glucose utilization and local cerebral blood flow (with an appendix on its statistical analysis). J Cereb Blood Flow Metab. 2:487–499.

Mintun MA, Lundstrom BN, Snyder AZ, Vlassenko AG, Shulman GL, Raichle ME. 2001. Blood flow and oxygen delivery to human brain during functional activity: theoretical modeling and experimental data. Proc Natl Acad Sci USA. 98:6859–6864.

Mogenson GJ, Jones DL, Yim CY. 1980. From motivation to action: functional interface between the limbic system and the motor system. Prog Neurobiol. 14:69–97.

Nehlig A, Coles JA. 2007. Cellular pathways of energy metabolism in the brain: is glucose used by neurons or astrocytes? Glia. 55: 1238–1250.

Pourtois G, Vuilleumier P. 2006. Dynamics of emotional effects on spatial attention in the human visual cortex. Prog Brain Res. 156:67–91.

Raczkowski D, Kalat JW, Nebes R. 1974. Reliability and validity of some handedness questionnaire items. Neuropsychologia. 12:43–47.

Ragland JD, Glahn DC, Gur RC, Censits DM, Smith RJ, Mozley PD, Alavi A, Gur RE. 1997. PET regional cerebral blood flow change during working and declarative memory: relationship with task performance. Neuropsychology. 11:222–231.

Raichle ME. 1998. Behind the scenes of functional brain imaging: a historical and physiological perspective. Proc Natl Acad Sci USA. 95:765–772.

Raichle ME, MacLeod AM, Snyder AZ, Powers WJ, Gusnard DA, Shulman GL. 2001. A default mode of brain function. Proc Natl Acad Sci USA. 98:676–682.
Raichle ME, Snyder AZ. 2007. A default mode of brain function: a brief history of an evolving idea. Neuroimage. 37:1083–1090.
Reivich M. 1974. Blood flow metabolism couple in brain. Res Publ Assoc Res Nerv Ment Dis. 53:125–140.
Reivich M, Alavi A, Wolf A, Fowler J, Russell J, Arnett C, MacGregor RR, Shiue CY, Atkins H, Anand A, et al. 1985. Glucose metabolic rate kinetic model parameter determination in humans: the lumped constants and rate constants for [18F]fluorodeoxyglucose and [11C]deoxyglucose. J Cereb Blood Flow Metab. 5:179–192.
Sawle GV, Hymas NF, Lees AJ, Frackowiak RS. 1991. Obsessional slowness. Functional studies with positron emission tomography. Brain. 114:2191–2202.
Schmahmann JD, Pandya DN. 1995. Prefrontal cortex projections to the basilar pons in rhesus monkey: implications for the cerebellar contribution to higher function. Neurosci Lett. 199:175–178.
Shulman GL, Astafiev SV, McAvoy MP, d'Avossa G, Corbetta M. 2007. Right TPJ deactivation during visual search: Functional significance and support for a filter hypothesis. Cereb Cortex [Epub ahead of print].
Siesjö BK. 1978. Cerebral energy metabolism. Chichester: Wiley.
Smith RJ, Karp KJ, Muehllehner G. 1994. The count rate performance of the volume imaging PENN-PET scanner. IEEE Trans Med Imaging. 13:610–618.
Smith RJ, Shao L, Freifelder R, Karp JS, Ragland JD. 1995. Quantitative measurements of cerebral blood flow in volume imaging PET scanners. IEEE Trans Nucl Sci. 42:1018–1023.
Sokoloff L. 1981. Relationship among local functional activity, energy metabolism, and blood flow in the central nervous system. Fed Proc. 40:2311–2316.
Wang GJ, Volkow ND, Felder C, Fowler JS, Levy AV, Pappas NR, Wong CT, Zhu W, Netusil N. 2002. Enhanced resting activity of the oral somatosensory cortex in obese subjects. Neuroreport. 13: 1151–1155.
Warach S, Gur RC, Gur RE, Skolnick BE, Obrist WD, Reivich M. 1987. The reproducibility of the 133Xe inhalation technique in resting studies: task order and sex related effects in healthy young adults. J Cereb Blood Flow Metab. 7:702–708.
Warach S, Gur RC, Gur RE, Skolnick BE, Obrist WD, Reivich M. 1992. Decreases in frontal and parietal lobe regional cerebral blood flow related to habituation. J Cereb Blood Flow Metab. 12: 546–553.